

A magnetic bald-patch flare in solar active region 11117

Chao-Wei Jiang^{1,2}, Xue-Shang Feng^{2,1}, Shi-Tsan Wu³ and Qiang Hu³

¹ Institute of Space Science and Applied Technology, Harbin Institute of Technology, Shenzhen 518055, China; chaowei@hit.edu.cn

² SIGMA Weather Group, State Key Laboratory for Space Weather, Center for Space Science and Applied Research, Chinese Academy of Sciences, Beijing 100190, China

³ Center for Space Plasma and Aeronomic Research, The University of Alabama in Huntsville, Huntsville, AL 35899, USA

Received 2017 April 15; accepted 2017 May 28

Abstract With *SDO* observations and a data-constrained magnetohydrodynamics (MHD) model, we identify a confined multi-ribbon flare that occurred on 2010 October 25 in solar active region 11117 as a magnetic bald patch (BP) flare with strong evidence. From the photospheric magnetic field observed by *SDO/HMI*, we find there are indeed magnetic BPs on the polarity inversion lines (PILs) which match parts of the flare ribbons. From the 3D coronal magnetic field derived from an MHD relaxation model constrained by the vector magnetograms, we find strikingly good agreement of the BP separatrix surface (BPSS) footpoints with the flare ribbons, and the BPSS itself with the hot flaring loop system. Moreover, the triggering of the BP flare can be attributed to a small flux emergence under the lobe of the BPSS, and the relevant change of coronal magnetic field through the flare is reproduced well by the pre-flare and post-flare MHD solutions, which match the corresponding pre- and post-flare AIA observations, respectively. Our work contributes to the study of non-typical flares that constitute the majority of solar flares but which cannot be explained by the standard flare model.

Key words: Sun: flares — Sun: corona — magnetic fields — magnetohydrodynamics (MHD) — methods: numerical

1 INTRODUCTION

It is commonly believed that solar flares are explosive manifestations of magnetic energy released in the solar atmosphere by magnetic reconnection (Shibata & Magara 2011). The magnetic energy can be stored in the solar corona by means of magnetic flux emergence and/or energy injection by photospheric surface motions (shear/twist) from the Sun's interior, and fast magnetic reconnection is the major process that releases stored energy. Depending on the specific coronal conditions, flares may be related or not to coronal mass ejections (CMEs). The eruptive flares, i.e., those accompanied with CMEs, are typically observed with two flare ribbons roughly parallel along the main polarity inversion line (PIL) of the magnetic field on the photosphere. These classical two-

ribbon flares have been extensively studied, converging to a well-known standard flare model (i.e., the CSHKP flare model, Carmichael 1964; Sturrock 1966; Hirayama 1974; Kopp & Pneuman 1976), in which an eruptive magnetic flux rope (MFR) rises above the PIL, stretches the overlying field lines, produces a vertical current sheet underneath and triggers reconnection there, which results in two-ribbon brightenings at the footpoints of the reconnecting field lines. Most of these flares occur in a common magnetic structure called a sigmoidal active region (AR), which is a manifestation of the sheared bipolar field and is favorable for formation of the MFR.

On the other hand, there are numerous flares, both eruptive and confined, that occur in a much more complicated manner than the classical two-ribbon flares. Flares associated with multiple ribbons that show complex pat-

terns have been frequently reported in recent observations, such as quasi-circular ribbon flares (Masson et al. 2009; Wang & Liu 2012), three-ribbon flares (Wang et al. 2014), X-shaped flares (Li et al. 2016; Liu et al. 2016) and remote flare ribbons distinct from the eruptive core site (or the secondary ribbon, e.g., Zhang et al. 2014). These atypical flares appear to be more difficult to explain as no standard model exists. However, considering that a very big portion of the flares are atypical, it is necessary to concentrate on study of these complex flares (Dalmasse et al. 2015).

The variety of flare-ribbon patterns is rooted in the complexity of the underlying, invisible coronal field. For instance, a closed circular-like ribbon is found to be produced by a coronal magnetic null-point configuration (Masson et al. 2009; Wang & Liu 2012; Jiang et al. 2013). To generally understand how flares occur, knowledge of where the reconnection might be triggered in a given configuration of the coronal field is required. Under typical coronal conditions, plasma resistivity is extremely low and the magnetic field is frozen into the plasma almost everywhere in the solar corona. As such, magnetic reconnection can only occur in certain places where the current forms thin layers for resistivity to be important to induce sufficient dissipation (Démoulin 2006, 2007). Such thin layers include magnetic separatrices and, more commonly, quasi-separatrix layers, across which the connectivity of field lines discontinues or changes abruptly, and consequently narrow, enhanced current sheets can easily form along there due to the photospheric driving motions (Priest & Forbes 2002; Titov et al. 2002; Longcope 2005).

Theoretical studies show that there are interesting places where coronal magnetic field lines become tangential to the photosphere at the PIL (e.g., Wolfson 1989; Low 1992; Titov et al. 1993). In such places, opposite to the normal case, the field line crosses the PIL from *negative* to *positive* polarity. These places are dubbed ‘bald patches’ (BPs) which have a visual appearance of a haircut with magnetic field lines being associated with hairs (Titov et al. 1993). Since the photosphere can be regarded as a line-tying boundary for the coronal field, a BP field line is thus very special because it is anchored at the BP in addition to its footpoints. As a result, the continuous set of BP field lines defines a separatrix surface (BPSS) of magnetic topology, across which the field-line linkage is discontinuous. This is rather important considering that a BP is the only place that can define magnetic

separatrices besides the case in which magnetic nulls are present in the corona. The field lines immediately above a BP are concave up (i.e., forming magnetic dips) and can hold material against solar gravity, which thus usually implies the existence of a filament associated with the BP (Titov & Démoulin 1999; Mackay et al. 2010). The criterion for the existence of BPs in the models of potential and linear force-free fields has been described in detail by Titov et al. (1993).

For the case of BPSS, current sheets are very prone to be formed and thus reconnection can be triggered by shearing motions at the photosphere footpoints of the BP-separatrix field lines or pushing by flux emergence under the BP-separatrix lobe. By a 3D numerical magnetohydrodynamics (MHD) simulation driven by a bottom shearing velocity, Pariat et al. (2009) showed that current can form all along the curved BP separatrices where the reconnection can take place successively. There is another possibility in which a vertical current sheet can be formed just above the BP due to a converging and upward movement of the field lines from different lobes (see fig. 1 in Titov et al. 1993). By this pinching effect, the two BP lobes are brought into contact and lead to a vertical current sheet formed between the oppositely directed magnetic fields, which eventually reconnect. Moreover, during the evolution of some magnetic configurations, BPs may be precursors of the emergence of a null point in the coronal field (Bungey et al. 1996), being again associated with reconnection processes. The BP separatrix also has a close relationship with MFR, which holds a central position in many flare/CME models (e.g., Forbes et al. 2006; Török & Kliem 2005; Kliem & Török 2006). During an MFR forming in the corona or emerging from below the photosphere, there might be a state when the MFR is bodily attached at the photosphere in addition to its two legs, and the BP separatrix is the interface between the MFR and the ambient field (Titov & Démoulin 1999). When viewed from above, this MFR-BPSS usually exhibits an S or inverse-S shape, and reconnection there can produce a hot plasma in corresponding field lines, which can explain the observations of coronal sigmoids. Indeed, Jiang et al. (2014) recently found an almost coincidence of an extreme ultraviolet (EUV) sigmoid in AR 11283 with the BPSS of a corresponding MFR reconstructed from an HMI vector magnetogram.

In terms of observation, BPs were first related to flares by Aulanier et al. (1998), who found a close correspondence between the BP separatrices and the $H\alpha$ and

X-ray emissions in a very small flare (or sub-flare) in AR 7722, which was firstly interpreted as a so-called ‘BP flare.’ Several observational studies also show that the reconnection triggered at a BP can be correlated with eruptive flares.

Delannée & Aulanier (1999) studied another example of a BP-related flare and CME near AR 8100 and AR 8102, and suggested that the eruption was triggered by reconnection occurring in a vertical current sheet, which is formed above the BP due to photospheric shearing motions and the line-tie condition at the BP (e.g., Titov et al. 1993). Wang et al. (2002) showed that in AR 8210 the emerging motion of a twist flux rope may drive a slow reconnection at a BP (manifesting as a flare), which removes the overlaying flux confining the flux rope to allow the flux rope to expand and form a CME. In addition, BPs are associated with a wider range of phenomena in the chromosphere and transition region, e.g., the transition region brightenings (Fletcher et al. 2001), in surge ejections and arch filament systems (Mandrini et al. 2002), and in Ellerman bombs, i.e., small-scale transient $H\alpha$ brightenings (Pariat et al. 2004). All these phenomena are closely related with flux emergence, which is frequently observed in the solar atmosphere.

However, it should be noted that, probably due to the lack of a high-resolution vector magnetogram or the rather small scale of the related flare, evidence for the existence of a BP in the aforementioned examples of a BP-flare was computed using an extrapolation of the photospheric field, particularly a linear extrapolation (e.g., the potential, linear force-free or linear magnetohydrostatic models) based only on the line-of-sight component of the photospheric field. Such kind of evidence is obviously very indirect and may not be reliable because of the limitation of the models, considering that the location of BPs can be deduced directly from vector magnetograms (with the 180° ambiguity resolved). Also it is very difficult to use a simple linear field model to recover the complex non-potential coronal structures, which are generally very nonlinear (e.g., Wiegelmann 2008), although on some occasions, the basic topology of the magnetic field can be ‘sketched’ roughly using linear models (Demoulin et al. 1997). To reconstruct the coronal field and capture the magnetic topology more precisely, it is necessary to use more realistic models, like the nonlinear force-free field (NLFFF) extrapolation or even the MHD model, with the photospheric vector field as input.

Now with high-resolution and high-cadence vector magnetic field data and EUV observations from *Solar Dynamics Observatory (SDO)*, we have more opportunity to test the theory of BP-induced flare. Very recently, based on a sophisticated topological analysis of NLFFF extrapolation from HMI vector magnetograms, Liu et al. (2014) suggested that magnetic reconnection at the BPSS may play an important role in producing an unorthodox X-class long-duration confined flare in AR 11339. In this paper we revisit a C-class confined flare event in AR 11117, which has been used for our validation of a conservation-element and solution-element (CESE)–MHD model for reconstructing a coronal magnetic field based on *SDO/HMI* vector magnetograms (Jiang et al. 2012). By analyzing the reconstructed magnetic field, we have preliminarily shown that there is a relation between this flare and a BP found on the vector magnetogram near the flare site and time. Here with the same modeling data we will give more concrete evidence of the correlation between the BP and the flare, and further show how magnetic reconnection at the BP is activated and investigate the corresponding change of the BP separatrices. The remainder of the paper is organized as follows.

In Section 2 we describe observations of the flare by *SDO/AIA* and in Section 3 we study the magnetic field on the photosphere and of the 3D topology, to provide evidence of the BP-flare and show how the flare is triggered. We finally discuss the results and conclude in Section 4.

2 OBSERVATIONS

As shown in Figure 1, the studied flare occurred in AR 11117 on 2010 October 25, when the AR was crossing the central meridian of the solar disk with latitude of 22°N . On this day, AR 11117 was the largest AR on the disk, and only one flare with class of C2.3 was recorded according to the *Geostationary Operational Environmental Satellite (GOES)* 1–8 Å light curve, which started at 22:06 UT, peaked at 22:12 UT and ended at about 22:18 UT. The AR consists of two leading sunspots of negative polarity, one in the north and the other in the south, followed by an elongated positive polarity in the east, and fast magnetic flux emergence to the core of the region during the day (denoted by the box in Fig. 1(c)). However, rather unexpectedly, the flare did not happen in the flux emerging site with strong magnetic shear, but in the intermediate region between the sunspots (in particular much closer to the north sunspot, which is further away from the flux emergence site than

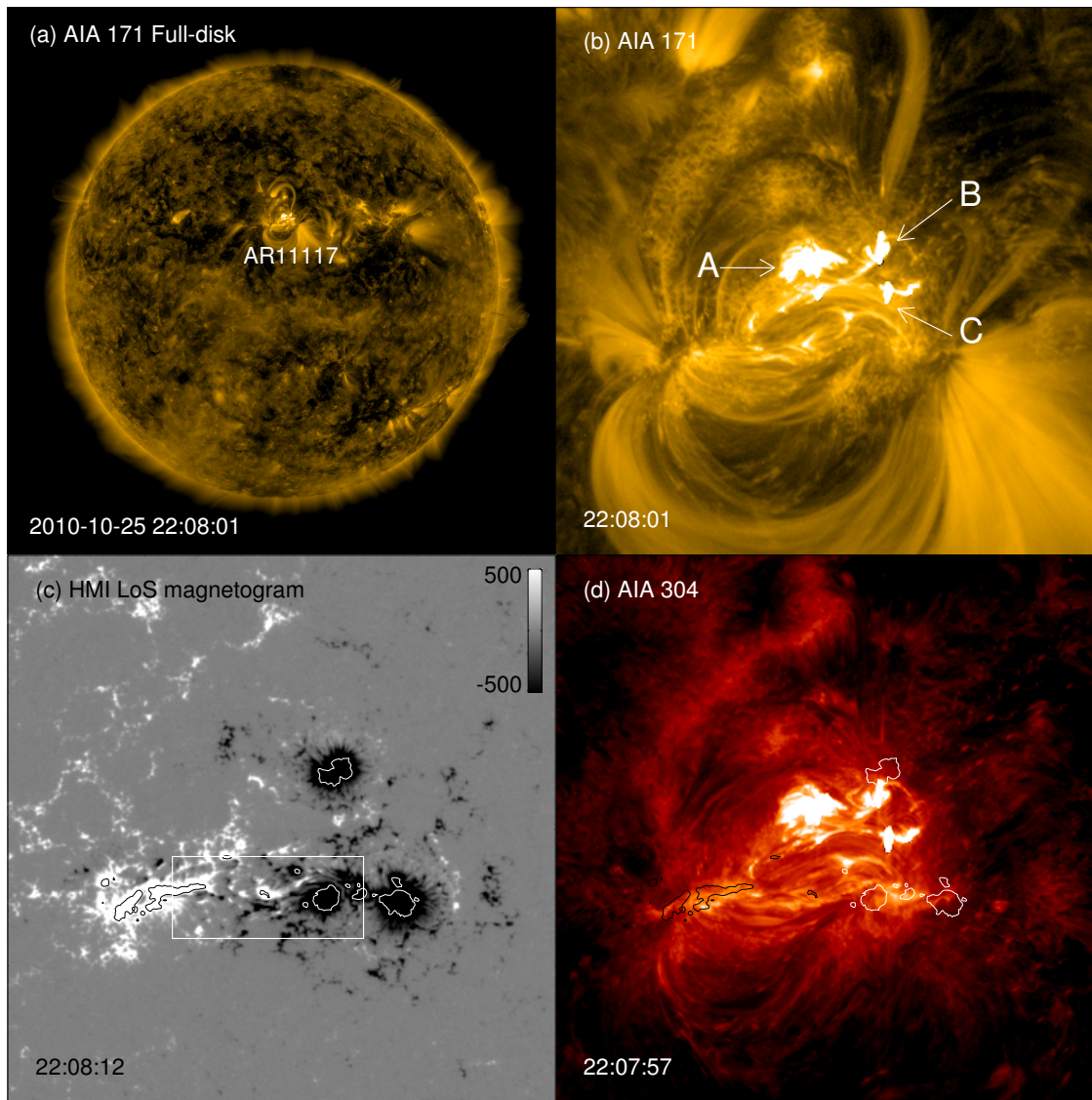


Fig. 1 Locations of AR 11117 and the flare site. (a) Full-disk *SDO/AIA* 171 Å image with AR 11117 outlined by the white rectangle on the image. (b) Enlarged view of AR 11117 in the full-disk image. The flare site with mainly three brightening kernels is labeled as A, B and C. (c) The HMI line-of-sight magnetogram with the same field-of-view as (b). Contour lines are plotted at ± 1000 G. The box region denotes a fast flux emergence site. (d) The AIA 304 Å image of the same region with contour lines in (c) overlapped on the image.

the south one, see Fig. 1(b) and (d)), where the field is relatively weak and no distinct magnetic shear is observed.

As recorded well by the AIA, the flaring process is confined in a rather low altitude without inducing major changes in the coronal loops or eruptions. Figure 2 displays the evolution of the flare site in detail with four EUV channels, 171 Å for the corona and hot loops shown by 94 Å, 304 Å for the upper chromosphere and 1600 Å for the lower/middle chromosphere. It begins to brighten at 22:07 UT and ends at 22:15 UT. The flare brightening can be seen most clearly for several minutes around

the time 22:08 UT, which Figure 1 demonstrates. We only roughly regard it as consisting of three brightening kernels labeled as A, B and C on the AIA image (see Fig. 1(b)), since these small patches are very close to each other and seem to be connected. The brightening patch at the east, A, is much bigger than the other two, B and C, at the west, indicating that more energy is delivered at A. By carefully inspecting time series of the AIA images (Fig. 2) or time-lapse movies, it seems that the flare is first brightened at kernel A, where it might be activated or triggered, and then brightened at B and C,

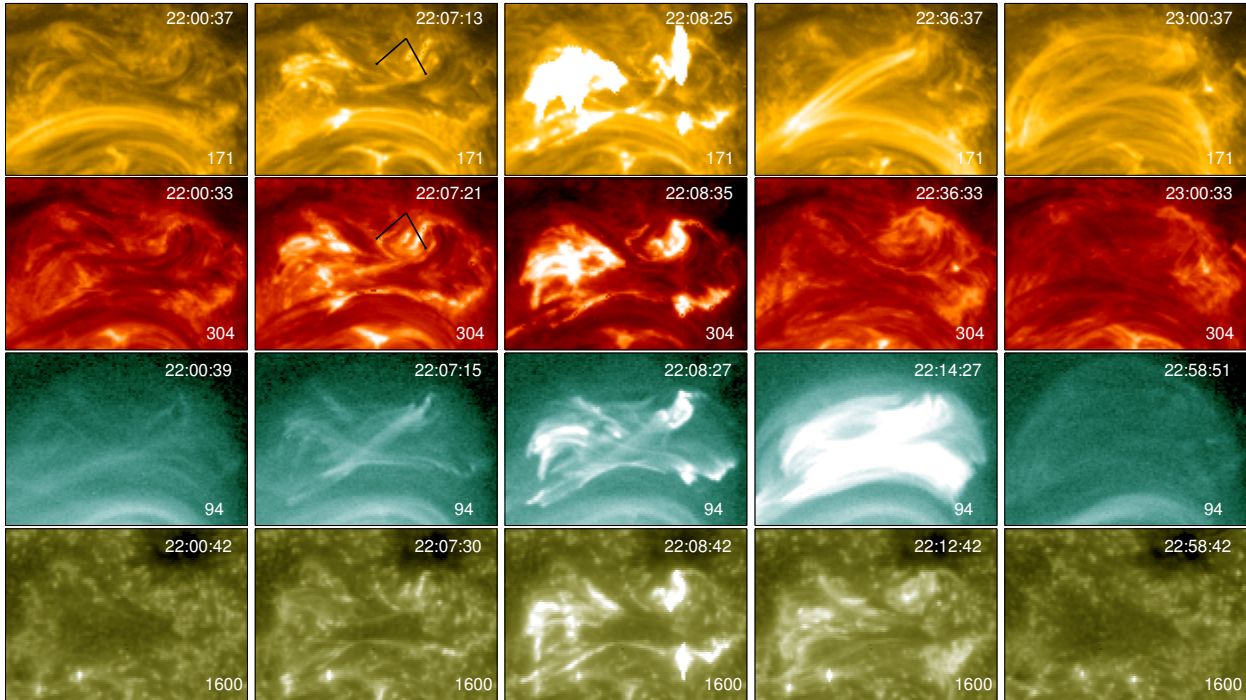


Fig. 2 Coronal evolution through the flare observed by AIA in channels of 171 Å, 304 Å, 94 Å and 1600 Å.

possibly because the energetic particles follow the magnetic field lines to their footpoints. Note that actually flare patch A consists of many even smaller patches by inspecting the 1600 Å images, indicating multiple complex footpoints of the coronal magnetic field are involved in reconnection.

As shown by the arrows on the AIA images of 171 Å and 304 Å in Figure 2, there appears to be a small curved dark feature overlying the flare kernels, indicating that field lines there exhibit some dips to support this filament-like material. This mini-filament was sustained for hours before the onset of the flare, and disappeared after the flare (see the AIA images at time 23:00 UT). As can be seen in AIA 171 Å, there is a new set of coronal loops expanding after the flare, in just the same location of the mini-filament that disappeared.

3 STUDY OF THE MAGNETIC FIELD

In our previous work (Jiang et al. 2012, 2016a), we developed a data-constrained CESE–MHD model to reconstruct the 3D coronal magnetic field. The MHD model, based on the space-time CESE scheme, is designed to focus on the magnetic-field evolution and to consider a simplified solar atmosphere in gravity with a small plasma

β . Magnetic vector-field data derived from observations at the photosphere are inputted directly to constrain the model. By considering that for the studied event the coronal configuration changes are very limited and can be approximated by successive MHD equilibria, we have solved a time sequence of MHD equilibria based on a set of vector magnetograms taken by HMI around the time of the flare. The model and results have been given in detail in Jiang et al. (2012), which shows that the model successfully reproduces the basic structures of the 3D magnetic field, as supported by good visual similarity between the field lines and the coronal loops observed by AIA. Here our analysis is confined to the magnetic topology and its change is related with the local region of the flare site.

Even before inspecting the coronal field, we find there are indeed BPs on the photosphere. With the vector magnetogram, one can identify BPs directly by searching for locations satisfying

$$\begin{aligned} B_z &= 0 \text{ and } \mathbf{B} \cdot \nabla B_z > 0, \\ z &= 0 \text{ (i.e., on the photosphere)}. \end{aligned} \quad (1)$$

This equation characterizes portions of PILs where the horizontal field crosses from negative to positive B_z .

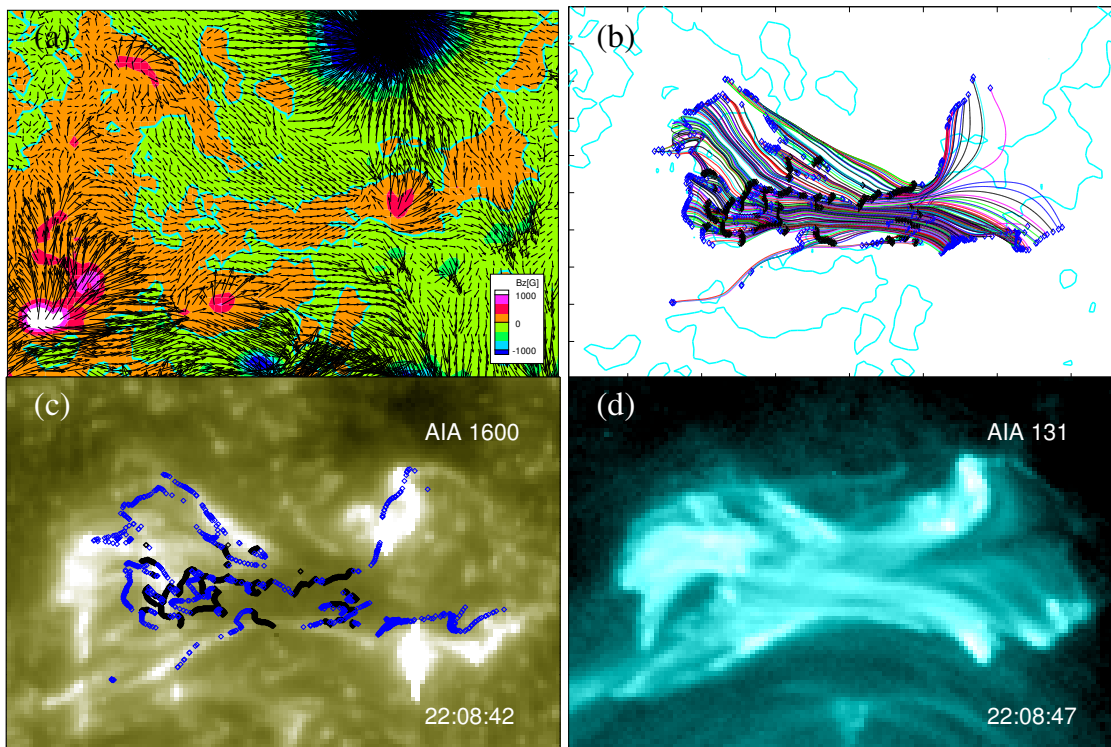


Fig. 3 Spatial relation between the flare site and the BPSS. (a) Magnetic vector fields at the photosphere are taken by HMI at 22:12 UT; (b) Magnetic field lines form the BPSS. The small diamond shapes in black denote the BPs, and those in blue are for the footpoints of the BPSS field lines. The thick cyan lines represent the photospheric magnetic PILs. (c) Flare brightening patches observed by AIA in 1600 Å, and overlaid are the BPs and BPSS footpoints. (d) Hot flaring loops observed by AIA in 131 Å.

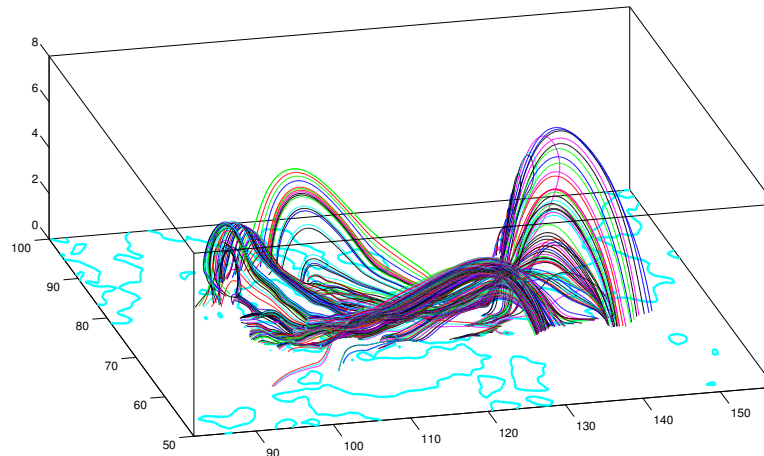


Fig. 4 3D view of the BPSS field lines as shown in Fig. 3(b).

SDO/HMI has taken a sequence of vector magnetograms with cadence of 12 min. Here we select the magnetogram taken at 22:12 UT, see Figure 3(a), which is mostly near the time of the flare. Locating the BPs is carried out on

a mesh refined by ten times from the original magnetogram using linear interpolation, and then we search for all the grid points fulfilling Equation (1). As shown in Figure 3(c), the BP points are plotted as black diamond

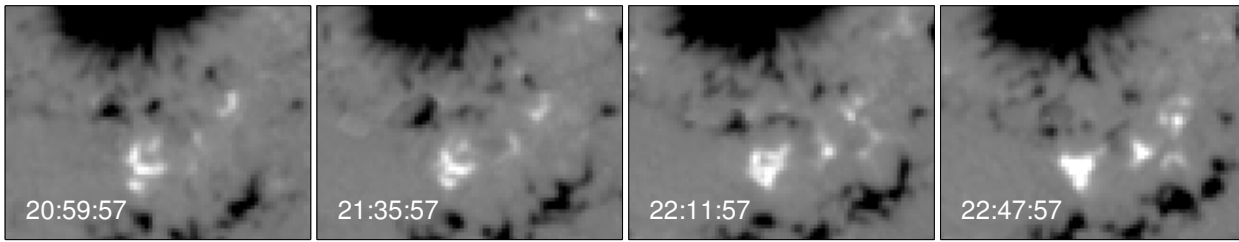


Fig. 5 Time sequence of HMI magnetograms shows a small emerging positive polarity under the west lobe of the BPSS.

shapes overlaid on the AIA-1600 image (the grid coordinates are co-aligned with the AIA image). Here it can be seen that the BP is clearly co-spatial with the flare location, mainly near flare patch A. The BPs mainly reside on the long PIL in the central region of the flare site (the thick cyan line on Fig. 3(b)), and there are some other small segments of BPs near this main PIL. On the main PIL, the BPs likely belong to a continuous long BP line, although they are disconnected frequently as derived from the observed vector field due to the noise of the magnetogram. One may worry about the reliability of the data since in this region the vector field is relatively weak (~ 200 G), but considering that the directions of the magnetic vectors do not show a pattern of random noise, we can be confident in the existence of these BPs.

We note that no BP coincides with flare patches B or C. Are these places related to the footpoints of the BPSS field lines? With the 3D coronal field model, we trace all the field lines passing through the BP points, which form the BPSS, and locate the footpoints of all these BPSS field lines. Figure 3(b) shows all these BPSS field lines, and their footpoints are marked as blue diamonds, which are also overlaid on the AIA-1600 image. As we have conjectured, the western BPSS footpoints are co-spatial and fit very well with the flare ribbon B and C, while the eastern footpoints coincide with flare patch A. A 3D view of the BPSS field lines is also shown in Figure 4, from which we can see that the apexes of the field lines are $3 \sim 4$ Mm, thus the whole structure is very low. The field lines outline the topology of the separatrix surface which separates three different topological regions. The footpoints in the east are very near the BPs, thus their brightenings along with those from the BPs produce the big flare patch A that consists of many even-smaller flare patches. Moreover, there should be another separatrix surface (not shown here) at the west of the BPs, which divides the west part into two connectivity domains and results in two different sets of footpoints, thus producing

the two flare patches B and C, respectively. Furthermore, comparing Figure 3(b) with (d) shows that the shape of the BPSS is in good agreement with the hot flaring loop observed in AIA-131, strongly suggesting that reconnection occurs in this BPSS and heats the plasma in corresponding field lines to form the hot loops. Moreover, the mini-filament as aforementioned (shown by arrows in Fig. 2) might be supported at the dips of field lines just above the BPSS. The disappearance of this mini-filament after the flare seems to suggest that the dipped field lines are lifted up by the magnetic reconnection at the BPSS, which make the field lines detached from the photosphere at the BP, and consequently the dense plasma is drained off by gravity. However, there is also a possibility that the disappearance of the mini-filament is because it was heated to a higher temperature insensitive to AIA-171 and 304 passbands.

With the above study based on the field at the time 22:12 UT, we have given strong evidence that the flare is co-related with the BP, and the process of the event is suggested as follows. Firstly magnetic reconnection is activated at the BP, then the accelerated particles there traced the field lines near the BP-separatrix and produced flare ribbons, and the field lines that are attached to the photosphere at the BP before the flare are lifted up by the reconnection and expand upward, manifesting by the emergence of the post-flare loops and the disappearance of the mini-filament. Such and similar processes can usually be related with flux emergence, which can trigger reconnection in the BPSS, for example in the formation of an AR (Pariat et al. 2004) and in the surges and arch filament systems (Mandrini et al. 2002).

In the present event, by inspecting the photospheric field evolution, we find that there is indeed an emergence of a small positive polarity under the west lobe of the BPSS, see Figure 5. With the evolution of the reconstructed magnetic field we are able to illustrate how the BPSS field lines evolve through the flare. The left panels

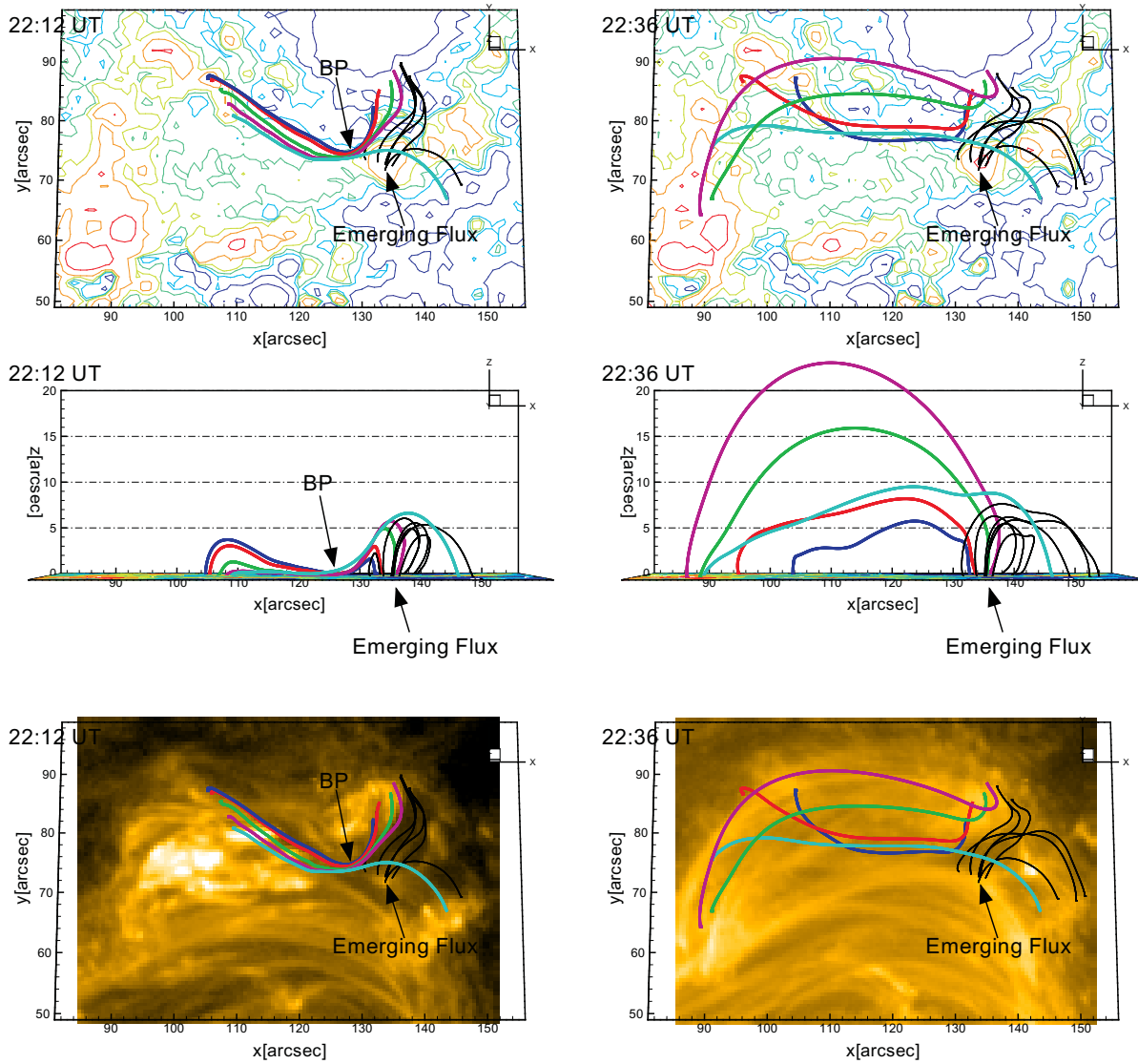


Fig. 6 Magnetic configuration change from pre-flare state (*left panels*) to post-flare state (*right panels*). The magnetic field lines are shown in *SDO* view angle (*top*) and side view (*middle*), and overlaid on *AIA-171* images (*bottom*). A group of BPSS field lines is shown in thick colored lines. Their footpoints in the west (*the right side*) are fixed for the pre-flare and post-flare field lines. A group of field lines from the emerging polarity are shown in black. The contour lines represent photospheric magnetogram B_z , red for positive and blue for negative.

of Figure 6 show several BPSS field lines (the colored thick lines) before the flare, while the right panels show their post-flare configuration. Under the west lobe of the BPSS, the emerging positive polarity is shown with a set of field lines (the black thick lines). The field lines rooted in the emerging flux expand upward (when comparing the post-flare state with the pre-flare state) and push the overlaying BPSS, which continuously increases electric currents in the BPSS and free energy to the system. When the current sheet is enhanced enough for resistivity to be

important, magnetic reconnection sets in at the BPSS, and the field lines attached at the BP by the photosphere plasma are lifted up, expanding as they relax, forming the post-flare loops. The field lines might also undergo slipping reconnection as they expand, with the footpoints not necessarily being in the same pre-flare locations. In the bottom panels, the field lines are overlotted on the *AIA-171* images, which demonstrate a nice agreement of the model field lines with the coronal loops.

4 CONCLUSIONS

In this study, we analyzed a C2.3 confined flare in AR 11117 with *SDO* observations and data-constrained MHD models. The flare is a non-standard case consisting of multiple ribbons, and it occurs in a region between the AR sunspots where the magnetic field is relatively weak and no distinct magnetic shear is observed, although the AR contains a typical fast emergence and strong-field site with significantly sheared PIL. With strong evidence, we concluded that this flare is triggered by magnetic reconnection in a BPSS and can be identified as a BP flare:

- (1) By directly inspecting the photospheric magnetic vector field measured by *SDO/HMI*, we find there are BPs on the PILs matching parts of the flare ribbons.
- (2) From the 3D coronal magnetic field derived from the MHD model constrained by vector magnetograms, we find strikingly good agreement of the BPSS footpoints with the flare ribbons, and the BPSS itself with the hot flaring loop system.
- (3) Moreover, the triggering of the BP flare can be attributed to a small flux emergence under the lobe of the BPSS, and the relevant change of the coronal magnetic field is well reproduced by the pre- and post-flare MHD solutions, which match the corresponding pre- and post-flare AIA observations. The flux emergence under the lobe of the BPSS triggers reconnection at the BP, making the pre-flare field lines that are attached to the photosphere at the BP relax and expand upward, and form the post-flare loops.

Our work contributes to the study of non-typical flares that constitute the majority of solar flares but which cannot be explained by the standard flare model. It is also worth noting that here the flare scenario is shown by MHD results constrained by observation data, and such data-constrained or even data-driven MHD modeling of the evolution of the coronal magnetic field is becoming a new and important approach for gaining a comprehensive understanding of the physical nature of non-typical flares (Jiang et al. 2016b).

Acknowledgements This work is jointly supported by the National Natural Science Foundation of China (41531073, 41374176, 41574170, 41231068 and 41574171) and the Specialized Research Fund for State

Key Laboratories. Data from observations are courtesy of NASA *SDO/AIA* and the HMI science teams.

References

- Aulanier, G., Démoulin, P., Schmieder, B., Fang, C., & Tang, Y. H. 1998, *Sol. Phys.*, 183, 369
- Bungey, T. N., Titov, V. S., & Priest, E. R. 1996, *A&A*, 308, 233
- Carmichael, H. 1964, *NASA Special Publication*, 50, 451
- Dalmasse, K., Chandra, R., Schmieder, B., & Aulanier, G. 2015, *A&A*, 574, A37
- Delannée, C., & Aulanier, G. 1999, *Sol. Phys.*, 190, 107
- Démoulin, P. 2006, *Advances in Space Research*, 37, 1269
- Démoulin, P. 2007, *Advances in Space Research*, 39, 1367
- Démoulin, P., Bagala, L. G., Mandrini, C. H., Henoux, J. C., & Rovira, M. G. 1997, *A&A*, 325, 305
- Fletcher, L., López Fuentes, M. C., Mandrini, C. H., et al. 2001, *Sol. Phys.*, 203, 255
- Forbes, T. G., Linker, J. A., Chen, J., et al. 2006, *Space Sci. Rev.*, 123, 251
- Hirayama, T. 1974, *Sol. Phys.*, 34, 323
- Jiang, C., Feng, X., Wu, S. T., & Hu, Q. 2012, *ApJ*, 759, 85
- Jiang, C., Feng, X., Wu, S. T., & Hu, Q. 2013, *ApJ*, 771, L30
- Jiang, C., Wu, S., & Feng, X. 2016a, *Frontiers in Astronomy and Space Sciences*, 3, 16
- Jiang, C., Wu, S. T., Feng, X., & Hu, Q. 2014, *ApJ*, 786, L16
- Jiang, C., Wu, S. T., Feng, X., & Hu, Q. 2016b, *Nature Communications*, 7, 11522
- Kliem, B., & Török, T. 2006, *Physical Review Letters*, 96, 255002
- Kopp, R. A., & Pneuman, G. W. 1976, *Sol. Phys.*, 50, 85
- Li, Y., Qiu, J., Longcope, D. W., Ding, M. D., & Yang, K. 2016, *ApJ*, 823, L13
- Liu, R., Chen, J., Wang, Y., & Liu, K. 2016, *Scientific Reports*, 6, 34021
- Liu, R., Titov, V. S., Gou, T., et al. 2014, *ApJ*, 790, 8
- Longcope, D. W. 2005, *Living Reviews in Solar Physics*, 2, 7
- Low, B. C. 1992, *A&A*, 253, 311
- Mackay, D. H., Karpen, J. T., Ballester, J. L., Schmieder, B., & Aulanier, G. 2010, *Space Sci. Rev.*, 151, 333
- Mandrini, C. H., Démoulin, P., Schmieder, B., Deng, Y. Y., & Rudawy, P. 2002, *A&A*, 391, 317
- Masson, S., Pariat, E., Aulanier, G., & Schrijver, C. J. 2009, *ApJ*, 700, 559
- Pariat, E., Aulanier, G., Schmieder, B., et al. 2004, *ApJ*, 614, 1099
- Pariat, E., Masson, S., & Aulanier, G. 2009, *ApJ*, 701, 1911
- Priest, E. R., & Forbes, T. G. 2002, *A&A Rev.*, 10, 313
- Shibata, K., & Magara, T. 2011, *Living Reviews in Solar Physics*, 8, 6
- Sturrock, P. A. 1966, *Nature*, 211, 695

- Titov, V. S., & Démoulin, P. 1999, *A&A*, 351, 707
- Titov, V. S., Hornig, G., & Démoulin, P. 2002, *Journal of Geophysical Research (Space Physics)*, 107, 1164
- Titov, V. S., Priest, E. R., & Demoulin, P. 1993, *A&A*, 276, 564
- Török, T., & Kliem, B. 2005, *ApJ*, 630, L97
- Wang, H., & Liu, C. 2012, *ApJ*, 760, 101
- Wang, H., Liu, C., Deng, N., *et al.* 2014, *ApJ*, 781, L23
- Wang, T., Yan, Y., Wang, J., Kurokawa, H., & Shibata, K. 2002, *ApJ*, 572, 580
- Wiegmann, T. 2008, *Journal of Geophysical Research (Space Physics)*, 113, A03S02
- Wolfson, R. 1989, *ApJ*, 344, 471
- Zhang, J., Li, T., & Yang, S. 2014, *ApJ*, 782, L27